This article has been accepted for publication in a future issue of this journal, but has not been fully edited. Content may change prior to final publication.
Citation information: DOI: 10.1109/TVT.2024.3359182, IEEE Transactions on Vehicular Technology

Energy-Efficient Covert Communications for UAV-Assisted Backscatter Systems

Yi Zhou, Azzam Al-nahari, Riku Jäntti, Zheng Ma, Pingzhi Fan

***Abstract*—In this paper, we propose an energy-efficient covert communication framework for UAV-assisted backscatter systems, where one UAV is deployed to collect data from one ground backscatter device (BD), in the presence of a warden who is trying to detect whether BD is transmitting or not. We first analyze the false alarm probability (FAP) and miss detection probability (MDP) for the covert communication and investigate the detection error probability by considering the location and channel uncertainty of warden. Then, aimed at maximizing the energy efficiency (EE) of our proposed system subject to reliability and covertness constraints, we optimize the UAV transmit power and hovering point jointly and design a low-complexity solution based on alternating optimization (AO), Dinkelbach method and successive convex approximation (SCA) solutions. Finally, simulation results are provided to verify the effectiveness of our proposed algorithm and highlight the fundamental trade-off between the EE and covertness constraint.**

***Index Terms*—UAV communications, backscatter communications, covert communications.**

I. Introduction

Backscatter communication, which empowers passive backscatter devices (BDs) to transmit signal by modulating radio-frequency carriers with low energy consumption and implementation cost, has been widely adopted in extensive Internet-of-Things (IoT) applications including smart agriculture, intelligent transportation and industrial automation [1]–[3]. Specifically, in bistatic backscatter communications, the signal transmitted from the carrier emitters (CEs) can be modulated and reflected by the passive BDs with their backscatter circuits, resulting in an expanded communication range of hundreds of meters [4]. In [5], a max-min energy efficiency fairness algorithm was developed for a wireless powered backscatter network with joint considerations of backscatter reflection coefficient and power beacon's transmission power.

Owing to its mobility and flexibility, unmanned aerial vehicle (UAV) which provides high-quality connectivity from the sky, has been recognized as one advanced aerial platform to assist backscatter communication [6]. The authors in [7] proposed a UAV-enabled backscatter communication framework where one UAV is deployed as data collector from multiple ground BDs, and investigated the fundamental trade-off between the UAV deployment and energy efficiency. In [8], to maximize the throughput in a UAV-assisted backscatter system, two protocols were designed by jointly optimizing the BD reflection coefficient, UAV trajectory and time allocation.

However, due to the broadcast nature of UAV air-to-ground channels, the UAV communications might be easily attacked by malicious adversaries, resulting in a series of harmful security threats, such as eavesdropping, malicious jamming and spoofing [9], [10]. To address the important security concerns, covert communication, which helps to hide the legitimate transmissions from being detected by malicious warden, has gained significant popularity recently [11], [12]. To maximize the average covert transmission rate for a UAV-enabled covert communications system, the authors in [13] optimized the UAV trajectory and transmit power jointly. In [14], a UAV-enabled covert transmission framework was established with the aid of intelligent reflecting surface. However, we note that only limited research attention has been focused on the covert communication in UAV-assisted backscatter communications system, thus strongly motivating this work.

Therefore, this paper aims at filling the above gap by proposing a new framework and its performance analysis. The main contributions of this paper are summarized as follows.

- An energy efficient covert communications framework for UAV-assisted backscatter systems is developed, where one UAV is deployed to collect data from one ground BD in the presence of a malicious warden.
- The explicit expressions for the false alarm probability (FAP) and miss detection probability (MDP) are derived, and the detection error probability is investigated by considering the location and channel uncertainty of warden.
- By jointly optimizing the UAV transmit power and hovering point, an energy efficiency (EE) maximization

Y. Zhou, Z. Ma and P. Fan are with the Provincial Key Lab of Information Coding and Transmission, Southwest Jiaotong University, Chengdu 610031, China. (e-mail: yizhou@swjtu.edu.cn; zma@swjtu.edu.cn; pzfan@swjtu.edu.cn).

Azzam Al-nahari is with the Department of Information and Communications Engineering, Aalto University, 02150 Espoo, Finland, and also with the Department of Electrical Engineering, Ibb University, Ibb, Yemen (e-mail: azzamyn@gmail.com).

Riku Jäntti is with the Department of Information and Communications Engineering, Aalto University, 02150 Espoo, Finland, (e-mail: riku.jantti@aalto.fi).

This work was supported in part by the National Natural Science Foundation of China under Grant U23A20274, 62361136810, 62301462, U2268201, 62271419, in part by the Young Elite Scientists Sponsorship Program by CAST under Grant 2022QNRC001, in part by Sichuan Science and Technology Program under Grant 2023YFG0321, in part by the Fundamental Research Funds for the Central Universities under Grant 2682023ZTPY060, in part by the European Project Hexa-X II, and in part by the Business Finland Project 6G-eMTC. The views and opinions expressed are however those of the authors only and do not necessarily reflect the views of Hexa-X-II Consortium.

This article has been accepted for publication in a future issue of this journal, but has not been fully edited. Content may change prior to final publication.
Citation information: DOI: 10.1109/TVT.2024.3359182, IEEE Transactions on Vehicular Technology

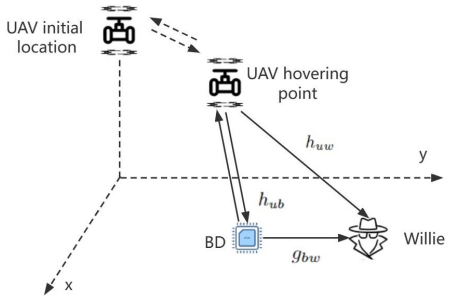

Fig. 1. Covert communications model for UAV-assisted backscatter systems.

solution with reliability and covertness considerations is proposed.

- Numerical results are provided to verify the effectiveness of our proposed EE maximization solution. Numerical results also highlight a fundamental trade-off between the EE and covertness constraint.

II. System Model and Problem Formulation

As shown in Fig. 1, we consider a UAV-assisted backscatter communication system where one UAV is deployed to collect data from one ground BD, in the presence of a warden (Willie) that is trying to detect whether BD is transmitting or not. We consider that the UAV moves from its initial location $(0,0)^T$ to the hovering point $\mathbf{u} = (x_u, y_u)^T$ with an average speed of v m/s in a fixed altitude H. Then, the UAV hovers at $\mathbf{u}$ for T_c seconds to collect data from the BD. The transmission of BD is based on the backscatter communications, where the UAV first transmits a single carrier signal to power up the BD, then, the BD adds the information onto the carrier signal and backscatters it to the UAV. When the collection process is completed, the UAV flies back to its initial location with a total flying time of $T_f = \frac{2||\mathbf{u}||}{v}$.

Denote the horizontal locations of BD and Willie as $\mathbf{r} = (x_b, y_b)^T$ and $\mathbf{y} = (x_w, y_w)^T$, respectively. Due to the strong line-of-sight (LoS) propagation of the UAV air-to-ground channels, we consider a pure distance-based model for UAV-BD and UAV-Willie links, which are denoted as h_{ub} and h_{uw}, respectively, and given by

$$h_{ub} = \sqrt{\frac{\Omega}{H^2 + ||\mathbf{u}-\mathbf{r}||^2}} \text{ and } h_{uw} = \sqrt{\frac{\Omega}{H^2 + ||\mathbf{u}-\mathbf{y}||^2}}, \quad (1)$$

where Ω represents the channel attenuation at unit reference distance. Moreover, for the BD-Willie link, we model it as $g_{bw} = h_{bw} f_{bw}$, where $h_{bw} = \sqrt{\frac{\Omega}{d_{bw}^{\kappa}}}$, $d_{bw} = ||\mathbf{r}-\mathbf{y}||$ is the distance between BD and Willie, and $\kappa > 2$ is the path loss component for terrestrial channels. In addition, we assume a Rayleigh fading channel for BD-Willie link and f_{bw} is the corresponding small-scale fading component.

A. Covert Communications

We assume that Willie knows the values of h_{ub} and h_{uw}. Moreover, from conservation perspective, we further assume that the instantaneous channel state information (CSI) of f_{bw} is known at Willie [4]. To detect whether BD is transmitting to the UAV or not, a hypothesis test based on the received signal is formulated at Willie, which is given by

$$y(i) = \begin{cases} \sqrt{P_c} h_{uw} s(i) + n_w(i), & H_0 \\ \sqrt{\alpha P_c} h_{ub} g_{bw} b(i) s(i) + \sqrt{P_c} h_{uw} s(i) + n_w(i), & H_1, \end{cases} \quad (2)$$

where $i = 1, 2, \cdots, k$ is the index of the subchannel and k is the total number of subchannels in each time slot. P_c is the transmit power at the UAV for communications and α is the reflection coefficient at the BD. Moreover, $s(i)$ and $b(i)$ represent the signals transmitted from the UAV and the BD in the i-th subchannel, respectively, with $\mathbb{E}[|s(i)|^2] = 1$ and $\mathbb{E}[|b(i)|^2] = 1$. Furthermore, $n_w(i) \sim \mathcal{CN}(0, \sigma_w^2)$ represents the additive white Gaussian noise (AWGN) at Willie in the i-th subchannel. The null hypothesis H_0 indicates that the BD is not transmitting while the alternative hypothesis H_1 represents that the BD is sending signals to the UAV.

Similar to [4] and [13], we formulate the statistic of the hypothesis test based on the average received power P, which is characterized as

$$P \triangleq \frac{1}{k} \sum_{i=1}^{k} |y(i)|^2 \underset{H_0}{\overset{H_1}{\gtrless}} \tau, \quad (3)$$

where τ is the detection threshold at Willie. Specifically, when k is sufficiently large, i.e., $k \to \infty$, P can be rewritten as [13]

$$P = \begin{cases} P_c |h_{uw}|^2 + \sigma_w^2, & H_0 \\ \alpha P_c |h_{ub}|^2 |g_{bw}|^2 + P_c |h_{uw}|^2 + \sigma_w^2, & H_1. \end{cases} \quad (4)$$

As in [13], we consider a bounded noise uncertainty model at Willie, where the exact noise power σ_w^2 lies in a finite range around a nominal noise power σ_n^2. We assume that $\sigma_{w,\mathrm{dB}}^2 \in [\sigma_{n,\mathrm{dB}}^2 - \varrho_{\mathrm{dB}}, \sigma_{n,\mathrm{dB}}^2 + \varrho_{\mathrm{dB}}]$ follows a uniform distribution in the dB domain, where $\sigma_{w,\mathrm{dB}}^2 = 10\log_{10}(\sigma_w^2)$, $\sigma_{n,\mathrm{dB}}^2 = 10\log_{10}(\sigma_n^2)$, and $\varrho_{\mathrm{dB}} = 10\log_{10}(\varrho)$ is a parameter that measures the size of the noise uncertainty. Thus, the distribution of σ_w^2 is given by

$$f_{\sigma_w^2}(x) = \begin{cases} \frac{1}{2\ln(\varrho)x}, & \frac{1}{\varrho}\sigma_n^2 \le x \le \varrho\sigma_n^2 \\ 0, & \text{otherwise.} \end{cases} \quad (5)$$

B. Detection Performance at Willie

To evaluate the detection performance, in this subsection, we derive the explicit expressions of FAP and MDP, which are defined as $P_{FA} = \Pr(H_1|H_0)$ and $P_{MD} = \Pr(H_0|H_1)$, respectively. As such, we have

$$P_{FA} = \begin{cases} 1, & \tau < \frac{\sigma_n^2}{\varrho} + P_c \left|h_{uw}\right|^2 \\ \theta_1, & \frac{\sigma_n^2}{\varrho} + P_c \left|h_{uw}\right|^2 \le \tau \le \varrho\sigma_n^2 + P_c \left|h_{uw}\right|^2 \\ 0, & \tau > \varrho\sigma_n^2 + P_c \left|h_{uw}\right|^2, \end{cases} \quad (6)$$

where

$$\theta_1 = \int_{\tau - P_c|h_{uw}|^2}^{\varrho\sigma_n^2} \frac{1}{2\ln(\varrho)x} dx = \frac{1}{2\ln(\varrho)} \ln\left(\frac{\varrho\sigma_n^2}{\tau - P_c|h_{uw}|^2}\right).$$

This article has been accepted for publication in a future issue of this journal, but has not been fully edited. Content may change prior to final publication.
Citation information: DOI: 10.1109/TVT.2024.3359182, IEEE Transactions on Vehicular Technology

Moreover, the MDP is given by

$$P_{MD} = \begin{cases} 0, & \tau < \frac{\sigma_n^2}{\varrho} + \eta \\ \theta_2, & \frac{\sigma_n^2}{\varrho} + \eta \leq \tau \leq \varrho\sigma_n^2 + \eta \\ 1, & \tau > \varrho\sigma_n^2 + \eta, \end{cases} \tag{7}$$

where $\eta = \alpha P_c |h_{ub}|^2 |g_{bw}|^2 + P_c |h_{uw}|^2$ and

$$\theta_2 = \int_{\frac{\sigma_n^2}{\varrho}}^{\tau-\eta} \frac{1}{2\ln(\varrho)x} dx = \frac{1}{2\ln(\varrho)} \ln\left(\frac{\varrho(\tau-\eta)}{\sigma_n^2}\right).$$

Based on (6) and (7), by considering equal probability of H_0 and H_1, we derive the expression of total error probability, i.e., $\zeta = P_{FA} + P_{MD}$, which is given by

$$\zeta = \begin{cases} 1, & \tau < \frac{\sigma_n^2}{\varrho} + P_c |h_{uw}|^2 \\ \theta_1 & \frac{\sigma_n^2}{\varrho} + P_c |h_{uw}|^2 \leq \tau < \frac{\sigma_n^2}{\varrho} + \eta \\ \theta_1 + \theta_2 & \frac{\sigma_n^2}{\varrho} + \eta \leq \tau \leq \varrho\sigma_n^2 + P_c |h_{uw}|^2 \\ \theta_2 & \varrho\sigma_n^2 + P_c |h_{uw}|^2 < \tau \leq \varrho\sigma_n^2 + \eta \\ 1 & \tau > \varrho\sigma_n^2 + \eta. \end{cases} \tag{8}$$

From Willie's perspective, the optimal threshold that minimizes the total error probability is discussed in the following lemma.

Lemma 1. *The optimal threshold that minimizes the total error probability at Willie is $\tau^* = \frac{\sigma_n^2}{\varrho} + \eta$ and the corresponding minimum total error probability is given by*

$$\zeta^* = \frac{1}{2\ln(\varrho)} \ln\left(\frac{\varrho\sigma_n^2}{\frac{\sigma_n^2}{\varrho} + \alpha P_c |h_{ub}|^2 |g_{bw}|^2}\right). \tag{9}$$

Proof. We note that ζ is monotonically decreasing with τ when $\frac{\sigma_n^2}{\varrho} + P_c |h_{uw}|^2 < \tau < \frac{\sigma_n^2}{\varrho} + \eta$. However, ζ is monotonically increasing with τ when $\frac{\sigma_n^2}{\varrho} + \eta \leq \tau < \varrho\sigma_n^2 + P_c |h_{uw}|^2$, and $\varrho\sigma_n^2 + P_c |h_{uw}|^2 < \tau \leq \varrho\sigma_n^2 + \eta$ since $\theta_1 + \theta_2 = \frac{1}{2\ln(\varrho)} \ln\left(\varrho^2 - \frac{\varrho^2 \alpha P_c |h_{ub}|^2 |g_{bw}|^2}{\tau - P_c |h_{uw}|^2}\right)$. As such, the optimal threshold that minimizes ζ is $\tau^* = \frac{\sigma_n^2}{\varrho} + \eta$ and the minimum total error probability is shown in (9). □

We note from (9) that the minimum error probability is independent of the direct distance between the UAV and Willie. However, it depends on the distances of the backscattering link and BD-Willie link.

C. Covertness Consideration from UAV's perspective

Since Willie may hide somewhere to keep itself secret to the UAV, it is challenging to obtain its precise geographical location and perfect CSI of BD-Willie link from UAV's perspective [13], [15]. As such, we consider a practical scenario that only imperfect Willie's location and CSI of the BD-Willie link are known at the UAV. First, to address the location uncertainty, we adopt a bounded location estimation error model with $\mathbf{y} \in \Theta \triangleq \{||\tilde{\mathbf{y}} - \mathbf{y}|| \leq \chi\}$, where $\tilde{\mathbf{y}}$ represents the estimated Willie's location and χ denotes the maximum location estimation error.

Next, to address the CSI uncertainty of BD-Willie link, we consider a bounded CSI estimation error model with $|f_{bw} - \tilde{f}_{bw}| \leq \delta$, where $\tilde{f}_{bw}$ represents the estimated CSI of BD-Willie link and δ denotes the maximum CSI estimation error.

To proceed, we consider the Willie's location and CSI of BD-Willie link that result in a lower bound of minimum detection error, which is given by

$$\zeta^{low} = \frac{1}{2\ln(\varrho)} \ln\left(\frac{\varrho\sigma_n^2}{\frac{\sigma_n^2}{\varrho} + \alpha P_c |h_{ub}|^2 |g_{bw}^{max}|^2}\right), \tag{10}$$

where $g_{bw}^{max} = h_{bw}^{max} f_{bw}^{max}$ with $f_{bw}^{max} = \tilde{f}_{bw} + \delta$ and $h_{bw}^{max} = \max_{\mathbf{y} \in \Theta} h_{bw} = \sqrt{\frac{\Omega}{||(\mathbf{r} - \tilde{\mathbf{y}}||-\chi)^\kappa}}$ when $\mathbf{y} = \tilde{\mathbf{y}} + \frac{\mathbf{r} - \tilde{\mathbf{y}}}{||\mathbf{r} - \tilde{\mathbf{y}}||}\chi$.

D. Energy Efficiency (EE) Metric

When UAV collects data from BD, the signal-to-noise ratio (SNR) at the UAV can be expressed as

$$\gamma_b = \frac{\alpha P_c |h_{ub}|^4}{\sigma_u^2}, \tag{11}$$

where σ_u^2 is the noise power at the UAV. Since only passive components are included in BD's circuit, the noise at the BD can be ignored [8]. As such, the number of data that the UAV can collect is given by $S_{tot} = B\log_2(1 + \gamma_b)T_c$, where B is the bandwidth provided for the BD.

Moreover, we note that the consumed power at the UAV includes the powers for flying, hovering and transmitting, which are represented by P_f, P_{hov}, and P_c, respectively. Thus, the overall energy consumption E_{tot} is given by $E_{tot} = P_f T_f + (P_c + P_{hov})T_c$.

Next, we define the EE as the ratio between the number of collected data and the energy consumption at the UAV, which can be characterized as

$$\eta_{EE} = \frac{S_{tot}}{E_{tot}} = \frac{B\log_2(1 + \gamma_b)T_c}{P_f T_f + (P_c + P_{hov})T_c}. \tag{12}$$

E. Problem Formulation

In this work, we aim to maximize the EE of our proposed UAV-assisted backscatter communications system subject to reliability and covertness constraints. By jointly optimizing the UAV transmit power P_c and hovering point $\mathbf{u}$, we formulate the optimization problem as

$$\max_{P_c, \mathbf{u}} \eta_{EE} = \frac{B\log_2(1 + \gamma_b)T_c}{P_f T_f + (P_c + P_{hov})T_c} \tag{13a}$$

$$s.t.\ \gamma_b \geq \gamma_{th} \tag{13b}$$

$$\zeta^{low} \geq 1 - \epsilon. \tag{13c}$$

Specifically, (13b) is a constraint for reliability where the SNR at the UAV should be no less than a predefined threshold γ_{th}. Constraint (13c) ensures the covertness of the backscatter transmission.

III. EE Maximization Solution

In this section, an EE maximization solution is designed to solve Problem (13) by applying a number of mathematical methods. First, we adopt the alternating optimization (AO) method to decompose Problem (13) into two subproblems to solve UAV transmit power P_c and hovering point $\mathbf{u}$ in an iterative manner.

This article has been accepted for publication in a future issue of this journal, but has not been fully edited. Content may change prior to final publication.
Citation information: DOI: 10.1109/TVT.2024.3359182, IEEE Transactions on Vehicular Technology

A. UAV Transmit Power Subproblem

We first optimize P_c with fixed hovering point $\mathbf{u}$. Thus, the UAV transmit power subproblem can be formulated as

$$\max_{P_c} \ \eta_{EE} = \frac{B\log_2\left(1+\frac{\alpha P_c|h_{ub}|^4}{\sigma_u^2}\right)T_c}{P_f T_f + (P_c+P_{hov})T_c} \tag{14a}$$

$$s.t.\ P_c \geq \frac{\gamma_{th}\sigma_u^2}{\alpha|h_{ub}|^4} \tag{14b}$$

$$P_c \leq \frac{\sigma_n^2(\varrho^{2\epsilon}-1)}{\alpha\varrho|h_{ub}|^2|g_{bw}^{max}|^2}. \tag{14c}$$

We note that the optimization subproblem is feasible only if $\frac{\gamma_{th}\sigma_u^2}{\alpha|h_{ub}|^4} \leq \frac{\sigma_n^2(\varrho^{2\epsilon_1}-1)}{\alpha\varrho|h_{ub}|^2|g_{bw}^{max}|^2}$. Next, we investigate the optimal UAV transmit power P_c^* in the following lemma.

Lemma 2. *The optimal UAV transmit power P_c^* that maximizes EE is given by*

$$P_c^* = \left[\frac{D_0E_0 - T_c}{T_cD_0\mathcal{W}\left(\frac{D_0E_0-T_c}{T_ce}\right)} - \frac{1}{D_0}\right]_{P_0}^{P_1}, \tag{15}$$

where $[x]_{x_0}^{x_1} = \min\{\max\{x, x_0\}, x_1\}$, $\mathcal{W}(\cdot)$ is the Lambert-W function, $E_0 = P_fT_f + P_{hov}T_c$, $D_0 = \frac{\alpha|h_{ub}|^4}{\sigma_u^2}$, $P_0 = \frac{\gamma_{th}\sigma_u^2}{\alpha|h_{ub}|^4}$, $P_1 = \frac{\sigma_n^2(\varrho^{2\epsilon_1}-1)}{\alpha\varrho|h_{ub}|^2|g_{bw}^{max}|^2}$.

Proof. By taking the first-order derivative of the objective function η_{EE} in terms of P_c, we have

$$\frac{\partial\eta_{EE}}{\partial P_c} = \frac{f(P_c)}{(E_0+P_cT_c)^2}, \tag{16}$$

where $f(P_c) = BT_c\left(\frac{D_0(E_0+P_cT_c)}{(1+P_cD_0)\ln 2} - T_c\log_2(1+P_cD_0)\right)$. Next, to show the monotonicity of the objective function, we take the first-order derivative of $f(P_c)$ as

$$\frac{\partial f(P_c)}{\partial P_c} = -\frac{BT_cD_0^2(E_0+P_cT_c)}{(1+P_cD_0)^2\ln 2} \leq 0, \tag{17}$$

which demonstrates that $f(P_c)$ is a decreasing function with respect to P_c. Since $\underset{P_c=0}{f(P_c)} = \frac{BT_cD_0E_0}{\ln 2} > 0$ and $\underset{P_c\to\infty}{f(P_c)} < 0$, thus, there exists one unique point which satisfies $f(\hat{P}_c) = 0$, which corresponds to

$$\hat{P}_c = \frac{D_0E_0 - T_c}{T_cD_0\mathcal{W}\left(\frac{D_0E_0-T_c}{T_ce}\right)} - \frac{1}{D_0}. \tag{18}$$

It can be observed that the original objective function η_{EE} first increases with increasing P_c, until reaches the point where $f(\hat{P}_c) = 0$, and after this point, the objective function keeps decreasing with increasing P_c. By considering the constraints (14b) and (14c), the optimal UAV transmit power P_c^* can be obtained from $\hat{P}_c$, P_0 or P_1, as shown in (15). Thus, we complete the proof. □

B. UAV Hovering Point Subproblem

In this subsection, we optimize the UAV hovering point with given P_c. To facilitate the following analysis, we introduce an auxiliary variable t representing the upper bound of $(H^2+||\mathbf{u}-\mathbf{r}||^2)^2$, i.e., $t \geq (H^2+||\mathbf{u}-\mathbf{r}||^2)^2$. As such, the optimization problem can be rewritten as

$$\max_{\mathbf{u},t} \ \eta_{EE} = \frac{B\log_2\left(1+\frac{\alpha P_c\Omega^2}{\sigma_u^2 t}\right)T_c}{\frac{2P_f||\mathbf{u}||}{v} + (P_c+P_{hov})T_c} \tag{19a}$$

$$s.t.\ ||\mathbf{u}-\mathbf{r}||^2 \leq \frac{\Omega\sqrt{\alpha P_c}}{\sqrt{\gamma_{th}\sigma_u^2}} - H^2 \tag{19b}$$

$$||\mathbf{u}-\mathbf{r}||^2 \geq \frac{\Omega\alpha P_c\varrho|g_{bw}^{max}|^2}{\sigma_n^2(\varrho^{2\epsilon_1}-1)} - H^2 \tag{19c}$$

$$||\mathbf{u}-\mathbf{r}||^2 \leq \sqrt{t} - H^2. \tag{19d}$$

Though relaxed, solving Problem (19) is still challenging due to the fractional structure in (19a). To tackle this difficulty, similar to [16], we first transform the objective function as

$$\text{(19a)} \rightarrow BT_c\underbrace{\log_2\left(1+\frac{\alpha P_c\Omega^2}{\sigma_u^2 t}\right)}_{\mathcal{I}_0} - \mu\frac{2P_f||\mathbf{u}||}{v} - \mu U_0, \tag{20}$$

where μ is a non-negative multiplier that can be obtained by applying Dinkelbach method and $U_0 = (P_c+P_{hov})T_c$. With the aim of maximizing η_{EE}, we seek to transform (20) into concave function. To proceed, we adopt the successive convex approximation (SCA) solution to derive a concave lower bound expression of $\mathcal{I}_0$. Based on the first-order Taylor expansion, the corresponding lower bound $\mathcal{I}_0^{lb}$ is given by

$$\mathcal{I}_0^{lb} = \log_2\left(1+\frac{\alpha P_c\Omega^2}{\sigma_u^2 t[n]}\right) - \frac{\alpha P_c\Omega^2(t-t[n])}{t[n]^2\sigma_u^2(1+\frac{\alpha P_c\Omega^2}{\sigma_u^2 t[n]})\ln 2}, \tag{21}$$

where $t[n]$ is the value of t in the n-th iteration.

We note that (19b) and (19d) are convex and the non-convexity arises from (19c). Next, by applying the similar SCA solution, we transform the left-hand-side (LHS) of (19c) as

$$w_0 = ||\mathbf{u}[n]-\mathbf{r}||^2 + 2(\mathbf{u}[n]-\mathbf{r})^T(\mathbf{u}-\mathbf{u}[n]), \tag{22}$$

where $\mathbf{u}[n]$ is the value of $\mathbf{u}$ in the n-th iteration.

By doing so, the UAV hovering point subproblem can be reformulated as

$$\max_{\mathbf{u},t} \ BT_c\mathcal{I}_0^{lb} - \mu\frac{2P_f||\mathbf{u}||}{v} - \mu U_0 \tag{23a}$$

$$s.t.\ w_0 \geq \frac{\Omega\alpha P_c\varrho|g_{bw}^{max}|^2}{\sigma_n^2(\varrho^{2\epsilon_1}-1)} - H^2 \tag{23b}$$

$$\text{(19b), (19d)}.$$

Due to its convexity, Problem (23) can be solved efficiently by applying interior-point method.

C. Overall Algorithm

The proposed EE maximization solution is summarized in Algorithm 1 where the UAV transmit power and hovering point are jointly optimized. Since our solution results in a non-decreasing sequence of EE, our proposed Algorithm 1 is guaranteed to converge. Moreover, we note that the complexity of Algorithm 1 is dominated by that of Problem (23) since the UAV transmit power is solved with explicit expression. Thus, our proposed Algorithm 1 is with polynomial complexity of

This article has been accepted for publication in a future issue of this journal, but has not been fully edited. Content may change prior to final publication.
Citation information: DOI: 10.1109/TVT.2024.3359182, IEEE Transactions on Vehicular Technology

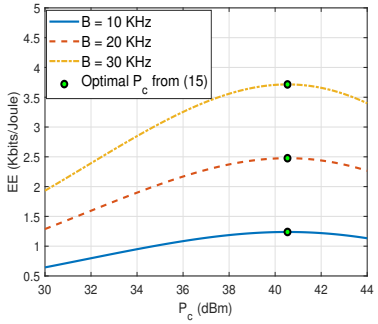

Fig. 2. EE versus UAV transmit power P_c.

$N_O N_I \mathcal{O}((3)^3)$, where N_O and N_I are the number of outer loop and inner loop iterations, respectively, and the base 3 represents the number of variables [17].

Algorithm 1 Proposed EE Maximization Solution for Problem (13).

1: Initialize: Set $P_c[0] = 3\ W, \mathbf{u}[0] = [280\ m, 0\ m]^T, \mu[0] = S_{tot}[0]/E_{tot}[0])$ and $n = 0$.
2: **repeat**(outer loop)
3: Update $P_c[n+1]$ based on (15);
4: **repeat**(inner loop)
5: Update $\mathbf{u}$ by solving Problem (23);
6: Update $\mu = BT_c\mathcal{I}_0^{lb}/(\frac{2P_f||\mathbf{u}||}{v} + U_0)$;
7: **until** convergence.
8: Update $\mathbf{u}[n+1]$;
9: Update the iterative number $n = n+1$;
10: **until** convergence.

IV. Numerical Results

In this section, numerical results are provided to highlight the effectiveness of our proposed EE maximization solution. We consider the BD and Willie are located at $\mathbf{r} = (300\ m, 25\ m)^T$ and $\mathbf{y} = (340\ m, 0\ m)^T$, respectively. The path loss component for terrestrial communication is set as $\kappa = 3$. We set $P_f = 30$ W, $P_{hov} = 8$ W, $|f_{bw}|^2 = 1.278$, $T_c = 40$ s, $\Omega = 10^{-2}$, $B = 10$ KHz, $\sigma_n^2 = -90$ dB, $\sigma_u^2 = -116$ dB, $\varrho_{dB} = 3$ dB, $\gamma_{th} = 3$ dB, $\epsilon = 0.01$, $H = 60$ m, and $\alpha = 1$. Moreover, we set the maximum location and CSI estimation errors as $\chi = 5$ m and $\delta = 10\%\tilde{f}_{bw}$.

In Fig. 2, we plot the relation between EE and the UAV transmit power P_c with different values of bandwidth. First, it can be seen that our analytical result of P_c in (15) leads to the maximum EE, which validates the accuracy of our derived solutions in Eq. (15). Next, we observe that a higher EE can be obtained with a larger bandwidth. This is intuitive since more data can be collected with a larger bandwidth without causing additional energy consumption, contributing to a higher EE. Specifically, when B increases from 10 KHz to 30 KHz, the maximum EE jumps from 1.238 Kbits/Joule to 3.715 Kbits/Joule, corresponding to a 200.08% EE increment.

In Fig. 3, the colormap of EE with different UAV hovering points is plotted. Specifically, in certain UAV hovering point, if either the reliability constraint or the covertness constraint cannot be satisfied, we set the corresponding EE as 0. Moreover, the BD's location and Willie's estimated location are represented by the purple circle and square, respectively. Several interesting observations can be found according to Fig. 3. First, if Willie is located at $(340\ \text{m}, 0\ \text{m})^T$ as shown in Fig. 3(a), when UAV hovers at any point in the target area, both the reliability and the covertness constraints can be satisfied. While as shown in Fig. 3(b), since Willie is located at $(320\ \text{m}, 0\ \text{m})^T$ and closer to the BD, there exists certain areas where the covertness constraint cannot be satisfied when UAV hovers in these regions.

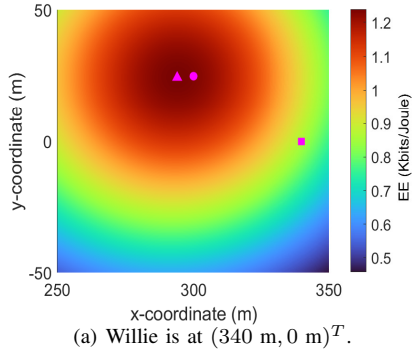

(a) Willie is at $(340\ \text{m}, 0\ \text{m})^T$.

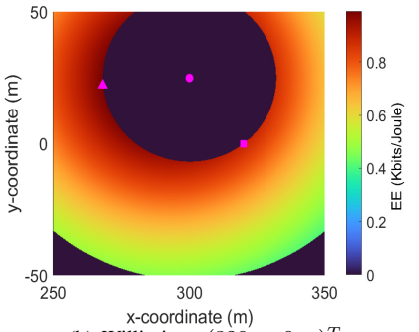

(b) Willie is at $(320\ \text{m}, 0\ \text{m})^T$.

Fig. 3. Colormap of EE. In certain point, if either the reliability constraint or the covertness constraint cannot be satisfied, the corresponding EE is set as 0.

Next, we can see from Fig. 3 that our derived UAV hovering point, which is obtained by adopting Algorithm 1 and represented by the purple triangle, results in a higher EE, thus verifying the correctness of our proposed solution. Specifically, when Willie is at $(340\ \text{m}, 0\ \text{m})^T$ as shown in Fig. 3(a), our derived UAV hovering point at $(294.00\ \text{m}, 24.49\ \text{m})^T$ results in a high EE of 1.24 Kbits/Joule. Moreover, when Willie is at $(320\ \text{m}, 0\ \text{m})^T$ as shown in Fig. 3(b), our derived UAV hovering point at $(268.10\ \text{m}, 22.30\ \text{m})^T$ results in a high EE of 0.99 Kbits/Joule. Moreover, according to Fig. 3(a), we observe that the optimal UAV hovering point is not at top of BD. This is because compared to the optimal UAV hovering point, when UAV is deployed at top of BD, even though a larger amount of collected data will be achieved due to the decreased distance between UAV and BD, the overall energy consumption increases as well since more energy is used for flying to the top of BD, resulting in a reduced EE.

This article has been accepted for publication in a future issue of this journal, but has not been fully edited. Content may change prior to final publication.
Citation information: DOI: 10.1109/TVT.2024.3359182, IEEE Transactions on Vehicular Technology

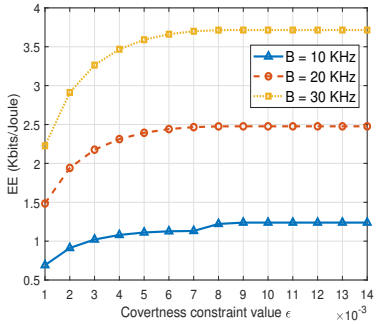

Fig. 4. EE versus different covertness constraint values ϵ.

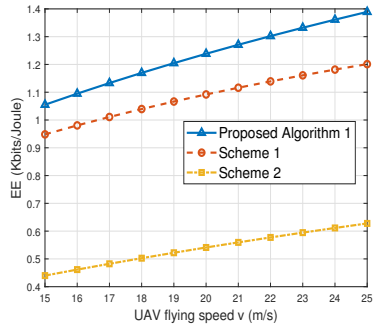

Fig. 5. Scheme comparison with different UAV flying speeds.

In Fig. 4, we plot the EE versus different covertness constraint values ϵ. We notice that the EE first increases with increasing ϵ until $\epsilon = 9 * 10^{-3}$, then it keeps unchanged with increasing ϵ. This is because with a more strict covertness constraint, i.e., $\epsilon \leq 8 * 10^{-3}$, the optimal UAV transmit power P_c is bounded by it, i.e. $P_1 < \hat{P}_c$. Thus, with increasing ϵ, the covertness constraint is relaxed and the EE is increased. When $\epsilon \geq 9 * 10^{-3}$, due to the loose covertness constraint, $\hat{P}_c \leq P_1$ is always satisfied and the EE performance cannot be increased by increasing ϵ.

To show the superiority of our proposed EE maximization solution, we consider the following two benchmark schemes.

- Scheme 1: Collected data maximization scheme, where the collected data maximization problem is formulated by removing the denominator of (13a);
- Scheme 2: Energy minimization scheme, where the energy minimization problem is formulated by minimizing the denominator of (13a).

According to Fig. 5, we observe that our proposed Algorithm 1 outperforms other benchmark schemes over a wide range of UAV flying speeds. Specifically, when $v = 25$ m/s, our Algorithm 1 achieves the highest EE of 1.389 Kbits/Joule, while that of Scheme 1 and Scheme 2 are 1.201 Kbits/Joule and 0.628 Kbits/Joule, respectively, at least improving 15.65% of the EE when compared to benchmark schemes.

V. Conclusions

In this paper, a covert communication framework was proposed in UAV-assisted backscatter system, where one UAV is deployed to collect data from one ground BD in the presence of a warden. To evaluate the detection performance, the explicit expression of detection error probability was derived by considering the location and channel uncertainty of the warden. Then, aimed at maximizing the EE subject to reliability and covertness constraints, a low-complexity iterative solution was designed by applying a series of mathematical methods. Numerical results verified the effectiveness of our proposed solution and highlighted the fundamental trade-off between EE and covertness constraint. For our future work, one possible extension is to consider mobile UAV with trajectory design in the presence of multiple BDs, which results in a more complicated optimization problem.

References

[1] W. Liu, Y. -C. Liang, Y. Li, and B. Vucetic, "Backscatter Multiplicative Multiple-Access Systems: Fundamental Limits and Practical Design," in *IEEE Trans. on Wireless Commun.,* vol. 17, no. 9, pp. 5713-5728, Sept. 2018.

[2] A. Al-Nahari, R. Jäntti, D. Mishra and J. Hämäläinen, "Massive MIMO Beamforming in Monostatic Backscatter Multi-Tag Networks," in *IEEE Commun. Lett.,* vol. 25, no. 4, pp. 1323-1327, April 2021.

[3] A. Al-Nahari, R. Jäntti, R. Duan, D. Mishra, and H. Yiğitler, "Multi-Bounce Effect in Multi-Tag Monostatic Backscatter Communications," in *IEEE Wireless Commun. Lett.* vol. 11, no. 1, pp. 43-47, Jan. 2022.

[4] Y. Wang, S. Yan, W. Yang, Y. Huang, and C. Liu, "Energy-Efficient Covert Communications for Bistatic Backscatter Systems," in *IEEE Trans. Veh. Technol.,* vol. 70, no. 3, pp. 2906-2911, March 2021.

[5] H. Yang, Y. Ye, and X. Chu, "Max-Min Energy-Efficient Resource Allocation for Wireless Powered Backscatter Networks," in *IEEE Wireless Commun. Lett.* vol. 9, no. 5, pp. 688-692, May 2020.

[6] G. Yang, R. Dai, and Y. -C. Liang, "Energy-Efficient UAV Backscatter Communication With Joint Trajectory Design and Resource Optimization," in *IEEE Trans. on Wireless Commun.,* vol. 20, no. 2, pp. 926-941, Feb. 2021.

[7] S. Yang, Y. Deng, X. Tang, Y. Ding, and J. Zhou, "Energy Efficiency Optimization for UAV-Assisted Backscatter Communications," in *IEEE Commun. Lett.,* vol. 23, no. 11, pp. 2041-2045, Nov. 2019.

[8] M. Hua, L. Yang, C. Li, Q. Wu, and A. L. Swindlehurst, "Throughput Maximization for UAV-Aided Backscatter Communication Networks," in *IEEE Trans. Commun.,* vol. 68, no. 2, pp. 1254-1270, Feb. 2020.

[9] Y. Zhou, P. L. Yeoh, H. Chen, Y. Li, R. Schober, L. Zhuo, and B. Vucetic,"Improving physical layer security via a UAV friendly jammer for unknown eavesdropper location," in *IEEE Trans. Veh. Technol.*, vol. 67, no. 11, pp. 11280-11284, Nov 2018.

[10] Y. Zhou, P. L. Yeoh, K. J. Kim, Z. Ma, Y. Li, and B. Vucetic, "Game Theoretic Physical Layer Authentication for Spoofing Detection in UAV Communications," in *IEEE Trans. Veh. Technol.,* vol. 71, no. 6, pp. 6750-6755, June 2022.

[11] M. Forouzesh, P. Azmi, A. Kuhestani, and P. L. Yeoh, "Covert Communication and Secure Transmission Over Untrusted Relaying Networks in the Presence of Multiple Wardens," in *IEEE Trans. Commun.,* vol. 68, no. 6, pp. 3737-3749, June 2020.

[12] X. Chen et al., "Covert Communications: A Comprehensive Survey," in *IEEE Commun. Surv. Tutor.,* vol. 25, no. 2, pp. 1173-1198, Secondquarter 2023.

[13] X. Zhou, S. Yan, J. Hu, J. Sun, J. Li, and F. Shu, "Joint Optimization of a UAV's Trajectory and Transmit Power for Covert Communications," in *IEEE Trans. Signal Process.,* vol. 67, no. 16, pp. 4276-4290, 15 Aug.15, 2019.

[14] C. Wang et al., "Covert Communication Assisted by UAV-IRS," *IEEE Trans. Commun.,* vol. 71, no. 1, pp. 357-369, Jan. 2023.

[15] X. Jiang, Z. Yang, N. Zhao, Y. Chen, Z. Ding, and X. Wang, "Resource Allocation and Trajectory Optimization for UAV-Enabled Multi-User Covert Communications," in *IEEE Trans. Veh. Technol.,* vol. 70, no. 2, pp. 1989-1994, Feb. 2021.

[16] A. J. Muhammed, Z. Ma, Z. Zhang, P. Fan, and E. G. Larsson, "Energy-Efficient Resource Allocation for NOMA Based Small Cell Networks With Wireless Backhauls," in *IEEE Trans. Commun.,* vol. 68, no. 6, pp. 3766-3781, June 2020.

[17] Y. Wu, W. Yang, X. Guan, and Q. Wu, "Energy-Efficient Trajectory Design for UAV-Enabled Communication Under Malicious Jamming," in *IEEE Wireless Commun. Lett.* vol. 10, no. 2, pp. 206-210, Feb. 2021.